Supporting Information (SI)

Revealing the interfacial water structure on a *p*-nitrobenzoic acid specifically adsorbed Au(111) surface

Yuan Fang,[a] Ren Hu,[b] Jin-Yu Ye,[b] Hang Qu,[c] Zhi-You Zhou,[b] Sai Duan,[a] Zhong-Qun Tian,[b] and Xin Xu[a,d*]

[a] Collaborative Innovation Center of Chemistry for Energy Materials (iChEM), Shanghai Key Laboratory of Molecular Catalysis and Innovative Materials, MOE Key Laboratory of Computational Physical Sciences, Department of Chemistry, Fudan University, Shanghai 200438, China.
[b] State Key Laboratory of Physical Chemistry of Solid Surfaces (PCOSS), Collaborative Innovation Centre of Chemistry for Energy Materials (iChEM), and Department of Chemistry, College of Chemistry and Chemical Engineering, Xiamen University, Xiamen 361005, China.
[c] Department of Chemistry and Materials Innovation Factory, University of Liverpool, 51Oxford Street, Liverpool L7 3NY, UK.
d.   Hefei National Laboratory, Hefei 230088, China.

*Corresponding author: xxchem@fudan.edu.cn (Xin Xu).

Contents:

Computational details
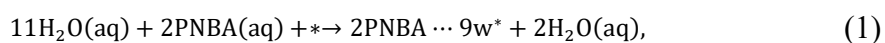
The metal surfaces were modelled as p(3×5) and p(2√3×2√3) Au(111) slabs with a lattice constant of 4.21 Å and a thickness of 7 layers in a periodic box of 79.45 Å (the middle three layers were frozen in the bulk position). The Au(111)(2√3×2√3) slab was used in the pure interfacial water system, and the Au(111)(3×5) slab was used in specific adsorption systems for PNBA⁻ and BS⁻ ions, PNBA and Py molecules. In the adsorption systems, the adsorbates were symmetrically coordinated with each side of the metal slab. All computations regarding the configurations were performed with VASP5.4.1 package.[1] The exchange-correlation energies were calculated using the alternative revision of the Perdew-Burke-Ernzerhof (RPBE) functional[2] with the generalized gradient approximation (GGA).[3] The dispersion correction was applied in all calculations with Becke-Johnson damping D3 method of Grimme, which was found to provide a more accurate and reliable description for various properties of water.[4] The electronic-ion interactions were described by the projector augmented wave method (PAW).[5] The pseudo-wave functions, the smooth part of the charge density and the potential were represented on 120×70×630 and 80×80×588 fast-Fourier-transform (FFT) meshes for the (3×5) and (2√3×2√3) unit cells, respectively. We considered a 550 eV plane-wave energy cut-off and sampled the surface Brillouin zone only with the Γ point. The self-consistent field procedure was repeated until reaching a precision of 1×10^{-9} eV in the total energy. All geometries were optimized to reach residual forces on all atoms lower than 0.01 eVÅ⁻¹. The simulated STM images were constructed on the basis of Tersoff-Hamann theory with a bias voltage of -0.09 V and were visualized using
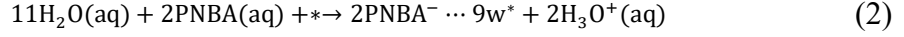
the p4vasp program.[6]

To calculate the EC-IR spectra, VASPsol implementation was employed to mimic the surface solvation effect.[7, 8] The relative permittivity ε_{re} and ionic strength I were set to 78 and 0.1 M (corresponding to a Debye screening length λ of 9.5 Å), respectively. The surface tension was set to zero (no cavitation energy). The finite difference method was employed to calculate IR spectra. The adsorbates at one side of the symmetric slab model and the outmost 4-layer metal atoms of the same side were frozen for the frequencies and spectral intensities calculation. The differential step size of Cartesian coordinates Δx was set to 0.01 Å. The calculated frequencies with respect to the measured ones were corrected by a scaling factor, 1.12. The calculated IR intensities were broadened by Lorentzian function with full width at the half-maximum (FWHM) of 20 cm^{-1} ($\upsilon < 1800$ cm^{-1}), and by Gaussian function with FWHM of 60 cm^{-1} ($\upsilon \geq 1800$ cm^{-1}). All calculated EC-IR spectra of combined Au(111)(3×5)-2PNBA with interfacial water configurations were referenced by the EC-IR spectrum of pure WL configuration at 0.34 V with a scaling factor of spectral intensity, 1.25.

Calculation of reaction free energy and hydrogen-bonding energy

Reaction free energies ΔG_{re} of all adsorption configurations were calculated to reference their Gibbs free energies G_{ads} to a unitary state.[9] The reference state was defined as two PNBA(aq) molecules, eleven H_2O(aq) molecules, and the bare Au(111) surface * in the implicit solvent. Accordingly, the reactions that form the adsorptions of 2PNBA···9w* and 2PNBA⁻···9w* from the reference state, were described as follows:

$$11H_2O(aq) + 2PNBA(aq) + * \rightarrow 2PNBA \cdots 9w^* + 2H_2O(aq), \tag{1}$$

$$11H_2O(aq) + 2PNBA(aq) + * \rightarrow 2PNBA^- \cdots 9w^* + 2H_3O^+(aq) \tag{2}$$

Therefore, the corresponding reaction free energies ΔG_{re} of the 2PNBA$\cdots$9w* and 2PNBA$^-\cdots$9w* were calculated by using Eqn. 3 and 4.

$$\Delta G_{re}^{2PNBA\cdots9W} = G_{ads}^{2PNBA\cdots9W} - G^* - 9G_{aq}^{H_2O} - 2G_{aq}^{PNBA}, \tag{3}$$

$$\Delta G_{re}^{2PNBA^-\cdots9W} = G_{ads}^{2PNBA^-\cdots9W} + 2G_{aq}^{H_3O^+} - G^* - 11G_{aq}^{H_2O} - 2G_{aq}^{PNBA} \tag{4}$$

Here, all computational details of potential-dependent Gibbs free energies of adsorption systems, molecules(aq), and ions(aq) were listed in ref. 10.

To deeply understand the contribution of hydrogen-bonding interactions, the potential-dependent energies E_{HB} of the single W$\cdots$W and PNBA$^-\cdots$W hydrogen-bonds in the adsorption configurations were calculated by using Eqn. 5 and 6.

$$E_{HB}^{W\cdots W} = [(G_{ads}^{2PNBA^-\&1W} - G_{ads}^{2PNBA^-}) + G_{ads}^{2PNBA^-\cdots8W} - G_{ads}^{2PNBA^-\cdots9W}]/N_{HB}^{W\cdots W}, \tag{5}$$

$$E_{HB}^{PNBA^-\cdots W} = [(G_{ads}^{9W} - G_{ads}^{8w}) + G_{ads}^{2PNBA^-\cdots8W} - G_{ads}^{2PNBA^-\cdots9W}]/N_{HB}^{PNBA^-\cdots W}, \tag{6}$$

Where the 2PNBA$^-\cdots$8W* indicated that a water molecule that was totally hydrogen-bonded with other water molecules or partly hydrogen-bonded with the adsorbed PNBA$^-$ was subtracted from the original adsorption configuration of the 2PNBA$^-\cdots$9W*; the 2PNBA$^-$* was just the Au(111)(3×5)-2PNBA$^-$ frame; the 2PNBA$^-$&1W* referred to the Au(111)(3×5)-2PNBA$^-$ frame plus the subtracted water molecule; the 9W* referred to the original adsorption configuration in the 2PNBA$^-\cdots$9W* by subtracting the adsorbed PNBA$^-$; the 8W* referred to the adsorption configuration in the 9W* by subtracting the water molecule that was partly hydrogen-bonded to the adsorbed PNBA$^-$; and the N_{HB} denoted the number of hydrogen-bonds in the W$\cdots$W or PNBA$^-\cdots$W for the specific water molecule in the original 2PNBA$^-\cdots$9W* adsorption

configurations.

Experimental details

The electrolyte solution, 0.1 M HClO$_4$, was prepared by diluting HClO$_4$ (Sigma, 311421) with Milli-Q water (> 18.2 MΩ·cm) and was deaerated with Ar gas before use. The concentration of *p*-nitrobenzoic acid (Sigma, 72910) was 1 mM. The chemical deposition of a 20 nm thick Au film on Si prism was performed according to the procedures and recipes reported by Miyake et al.[11] For the purpose of obtaining an ordered surface, the Au film was annealed using a butane flame and cooled subsequently in an air atmosphere.[12]

Electrochemical measurements were carried out with a potentiostat (EG&G, Model 263A). The chemically deposited and annealed Au film electrode (Ø=8 mm) was used as the working electrode. A saturated calomel electrode (SCE) was used as the reference electrode. All measurements were carried out after cycling the potential several times between 0 and 0.8 V *vs*. SCE to ensure a Au(111)-(1×1) surface. All potentials in this work, unless otherwise specified, were quoted against SHE, for comparison with data from first-principles calculations.

Infrared spectra of adsorbed species at the electrode surfaces were measured *in-situ* by using the Kretschmann ATR configuration[13]. Infrared radiation from a Nicolet 8700 spectrometer was shaded from the prism side at an incident angle of 60° and the totally reflected radiation was detected with a liquid-nitrogen cooled MCT detector. Spectra were acquired sequentially under potential step conditions. The spectral

resolution used was 8 cm^{-1}. All experimental EC-IR spectra were shown in absorbance units defined as -log(I/I_{ref}), where I and I_{ref} represent the intensities of the IR radiation at sample and reference potential (0.34 V vs. SHE).
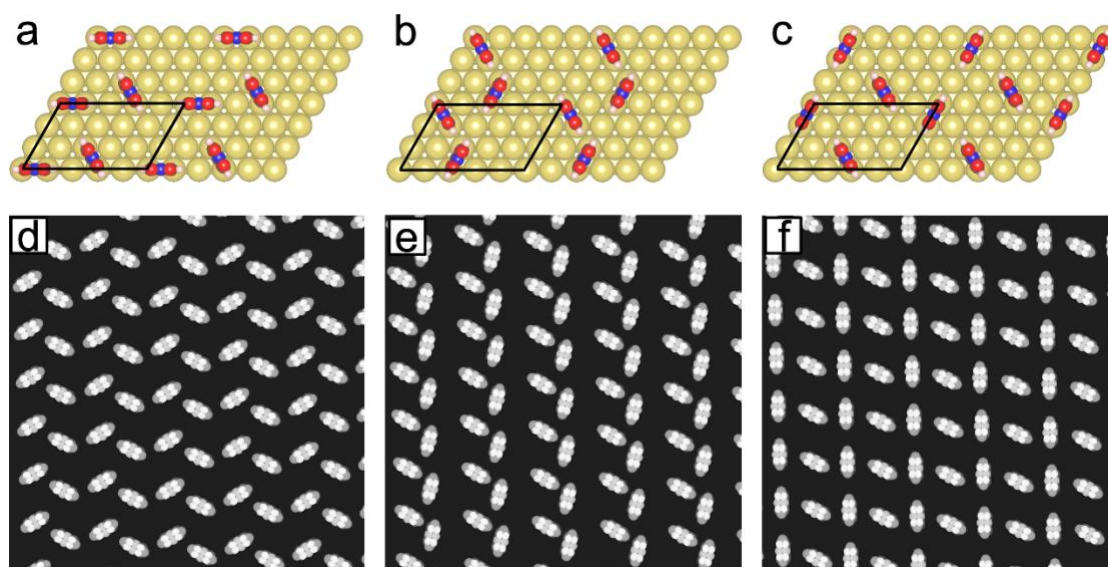
Fig. S1 Au(111)(3×5)-2PNBA⁻ configurations with specific angles θ between the a axis of (3×5) unit cell and the molecular plane of PNBA⁻ at the corners: (a) θ=0º, (b) θ=60º, and (c) θ=120º. Calculated STM images of (d) Au(111)(3×5)-2PNBA⁻(θ=0º), (e) Au(111)(3×5)-2PNBA⁻(θ=60º), and (f) Au(111)(3×5)-2PNBA⁻(θ=120º) configurations at 0.69 V *vs*. SHE. Gold, brown, pink, red, and blue balls denote Au, C, H, O, and N atoms, respectively.
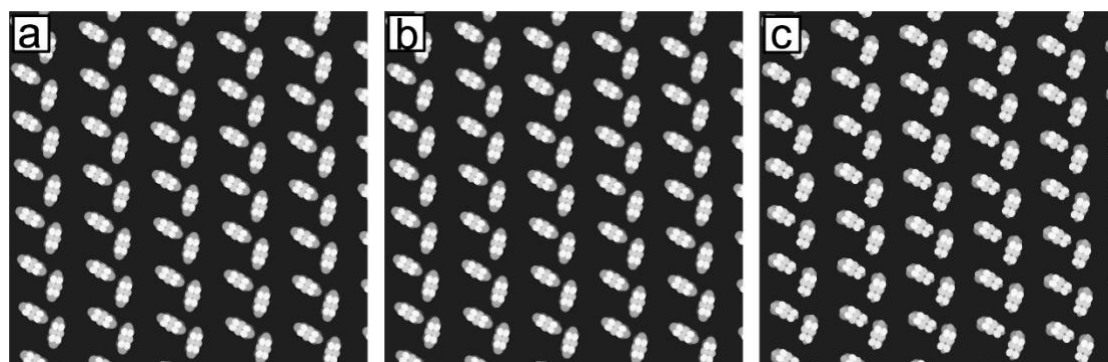
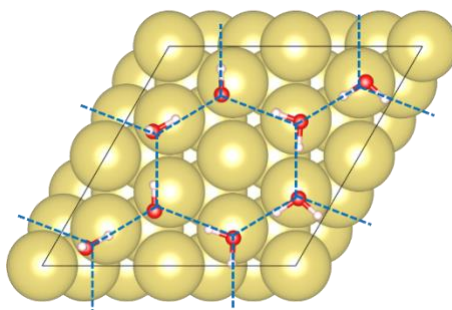**Fig. S2** Calculated STM images of (a) Ion-5MW, (b) 6M-Ion&W, and (c) Mol-5MW configurations at 0.69 V *vs*. SHE.

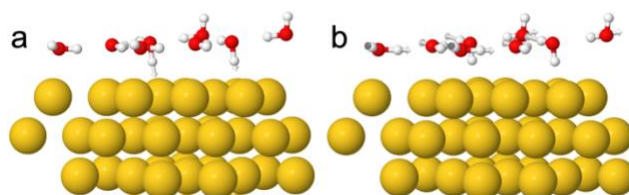**Fig. S3** The structure of the pure 1st WL configuration.

Fig. S4 Vibrational modes of the pure 1st WL configuration: (a) the OH stretching mode of the non-hydrogen-bonded water, $\nu^{NHB}(OH)$; (b) the OH stretching mode of water hydrogen-bonded with themselves, $\nu^{W\cdots W}(OH)$.
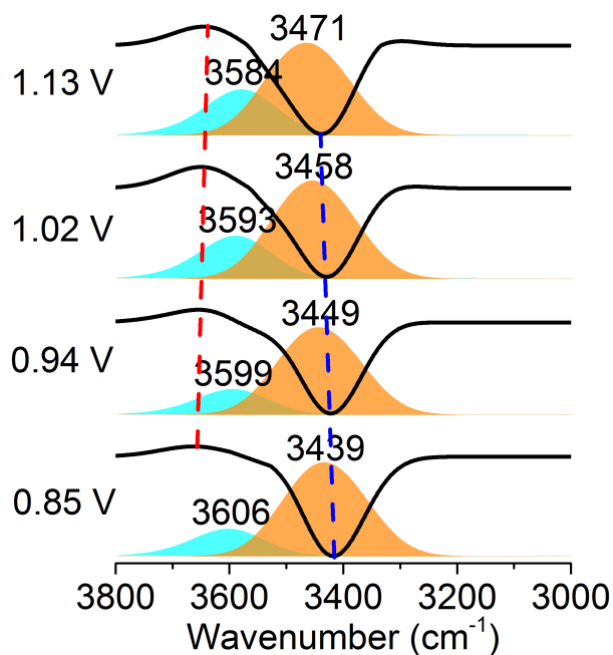

Fig. S5 Calculated EC-IR spectra of the Ion-5MW configuration in the Au(111)/PNBA solution interface at 0.85–1.13 V *vs*. SHE. The calculated EC-IR spectra have been referenced by the EC-IR spectrum of the pure WL configuration at 0.34 V. Orange and cyan flakes denote the contribution of the OH stretching mode $\nu(OH)$ of water molecules hydrogen-bonded with themselves and hydrogen-bonded to the PNBA⁻ ions, respectively.

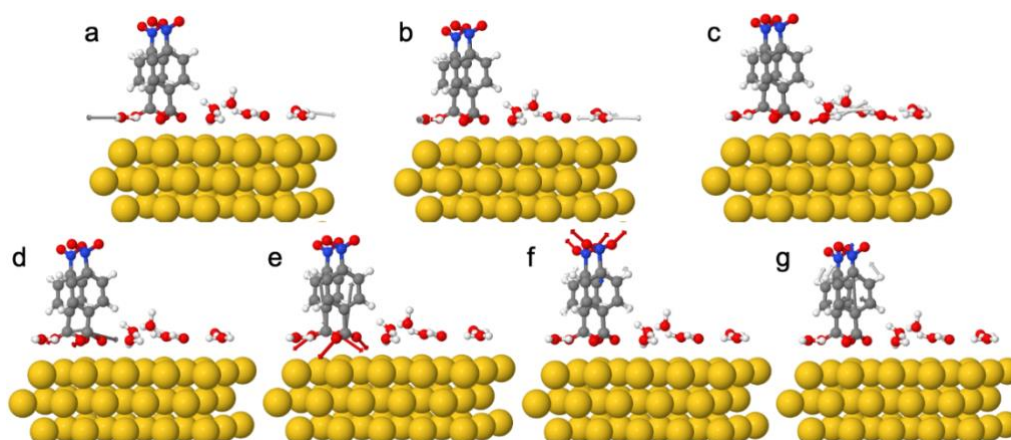**Fig. S6** Vibrational modes for the combined configuration of Au(111)(3×5)-2PNBA⁻ with 1st WL: (a) the OH stretching mode of water hydrogen-bonded with adsorbed PNBA⁻, $\nu^{PNBA^-\cdots W}(OH)$; (b)

the OH stretching mode of water hydrogen-bonded with themselves, $v^{W\cdots W}(OH)$; (c) the bending mode of water hydrogen-bonded with themselves, $\delta^{W\cdots W}(W)$; (d) the anti-symmetric CO_2 stretching mode for the adsorbed PNBA⁻, $v_{anti-sym}^{PNBA^-}(CO_2)$; (e) the symmetric CO_2 stretching mode for the adsorbed PNBA⁻, $v_{sym}^{PNBA^-}(CO_2)$; (f) the symmetric NO_2 stretching mode for the adsorbed PNBA⁻, $v_{sym}^{PNBA^-}(NO_2)$; (g) the CN stretching mode for the adsorbed PNBA⁻, $v^{PNBA^-}(CN)$.
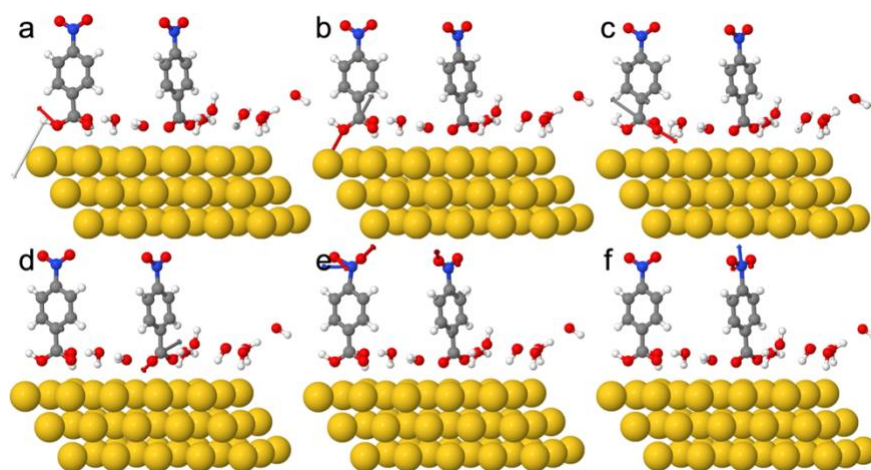

Fig. S7 Vibrational modes for the combined configuration of Au(111)(3×5)-2PNBA with 1st WL: (a) the asymmetric bending mode of carboxylate group for the adsorbed PNBA molecule, $\delta_{asym}^{PNBA}(COH)$; (b) and (c) Asymmetric CO_2 stretching modes for the adsorbed PNBA molecule, $v_{asym}^{PNBA}(CO_2)$; (d) the anti-symmetric CO_2 stretching mode for the adsorbed PNBA molecule, $v_{anti-sym}^{PNBA}(CO_2)$; (e) the anti-symmetric NO_2 stretching mode for the adsorbed PNBA molecule, $v_{anti-sym}^{PNBA}(NO_2)$; (f) the CN stretching mode for the adsorbed PNBA molecule, $v^{PNBA}(CN)$.
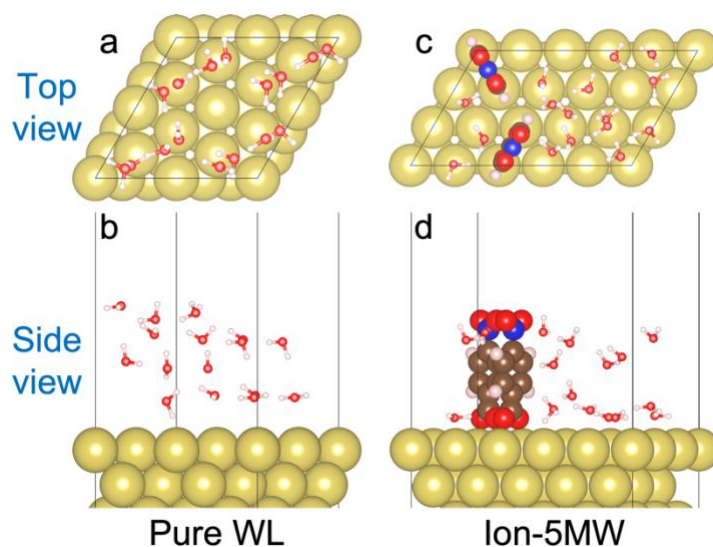

Fig. S8 The structure of the 1st+2nd WL on the bare Au(111) surface (a and b) and the PNBA⁻ ion adsorbed Au(111) surface (c and d).
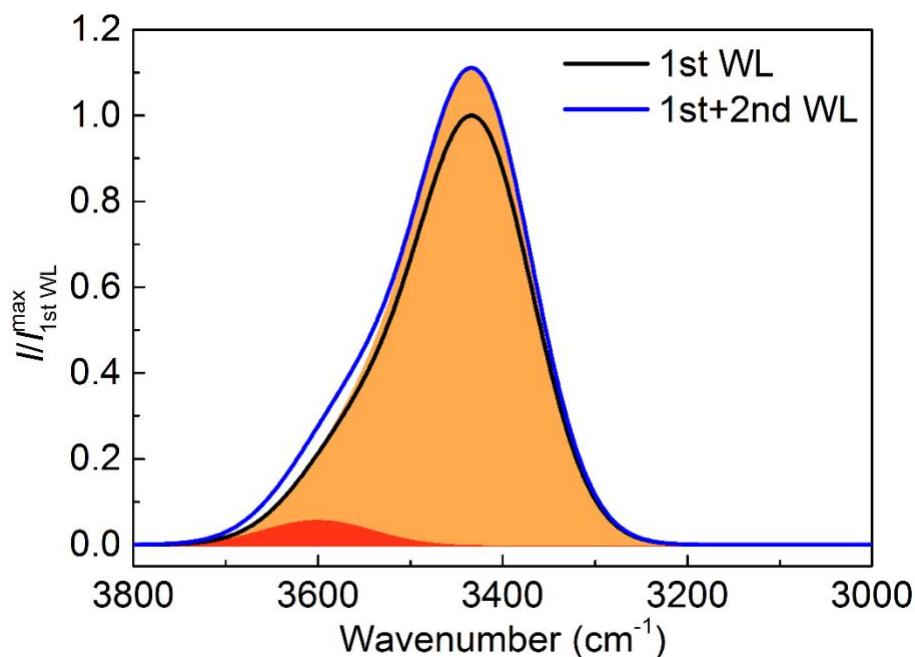
Fig. S9 Calculated EC-IR spectra for the pure 1st WL and the 1st+2nd WL configurations at 0.34 V vs. SHE from 3000 to 3800 cm^{-1} wavenumbers. Red and orange flakes denote the contribution of $\nu^{\text{NHB}}(\text{OH})$ and $\nu^{\text{W}\cdots\text{W}}(\text{OH})$ modes of the pure 1st+2nd WL configuration, respectively.
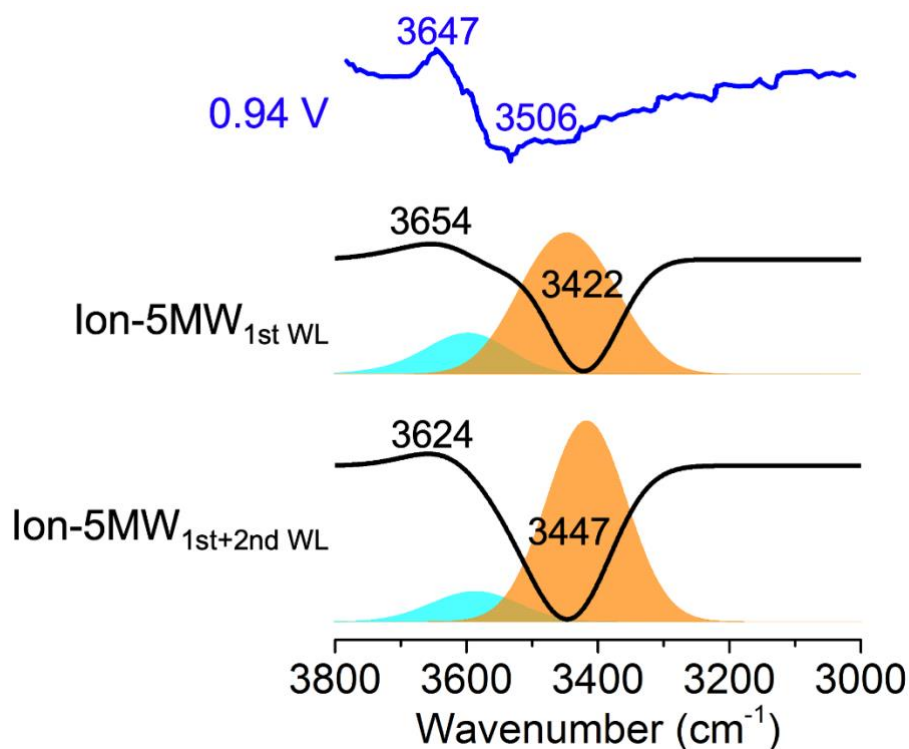

Fig. S10 Calculated EC-IR spectra for the Ion-5MW configurations with 1st WL, and 1st+2nd at 0.94 V *vs*. SHE from 3000 to 3800 cm^{-1} wavenumbers. The blue curve denotes the measured EC-IR spectra at 0.94 V. Cyan and orange flaks denote the contribution of $\nu^{\text{PNBA}^-\cdots\text{W}}(\text{OH})$ and $\nu^{\text{W}\cdots\text{W}}(\text{OH})$ modes, respectively.
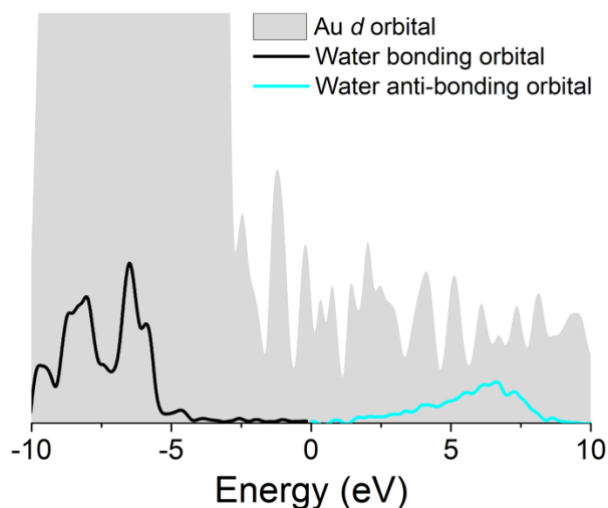
Fig. S11 pDOSs of the Ion-5MW combined configuration in the Au(111)/PNBA solution interface at 0.94 V *vs*. SHE. The Fermi level is located at 0 eV. The black curve, cyan curve, and gray flake region denote the bonding and the anti-bonding orbital of the water molecule and Au(111) surface *d* orbital, respectively.
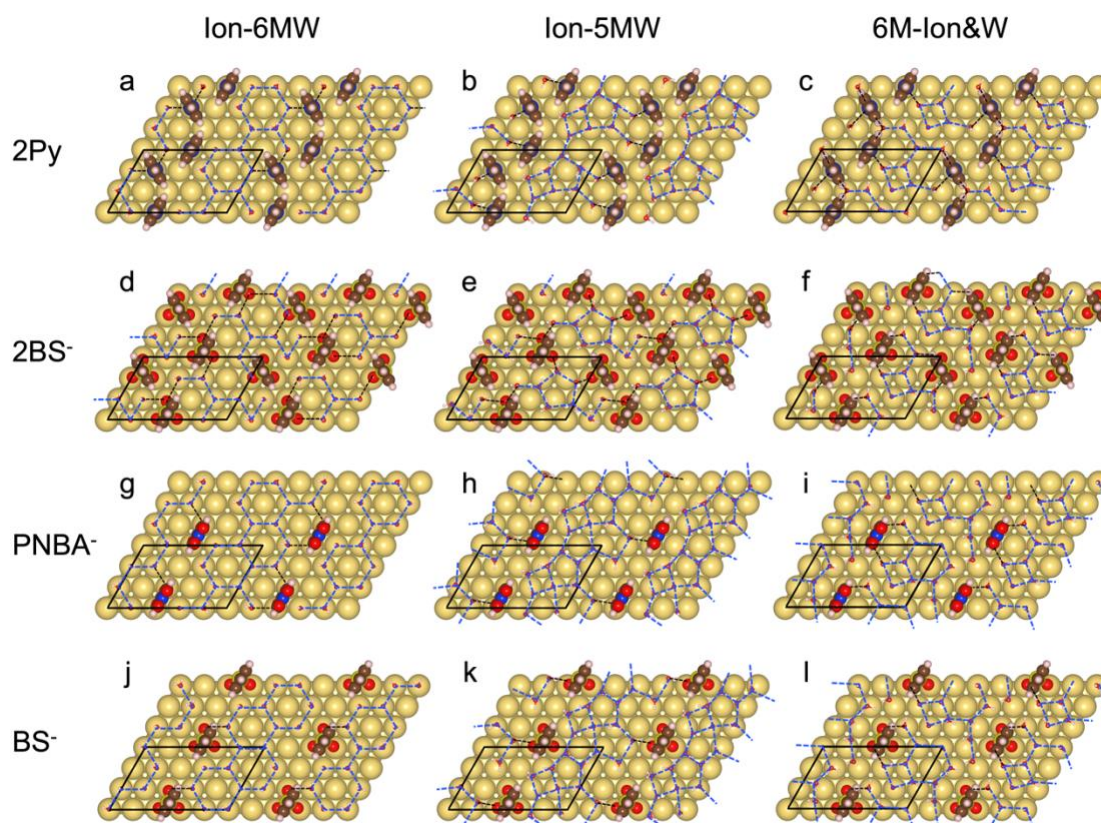

Fig. S12 Ion-6MW, Ion-5MW, and 6M-Ion&W configurations in the Au(111)(3×5) unit cell with different specifically adsorbed species: (a)–(c) 2Py, (d)–(f) 2BS⁻, (g)–(i) PNBA⁻, and (j)–(l) BS⁻. Gold, brown, pink, red, blue, and yellow balls denote Au, C, H, O, N, and S atoms, respectively.
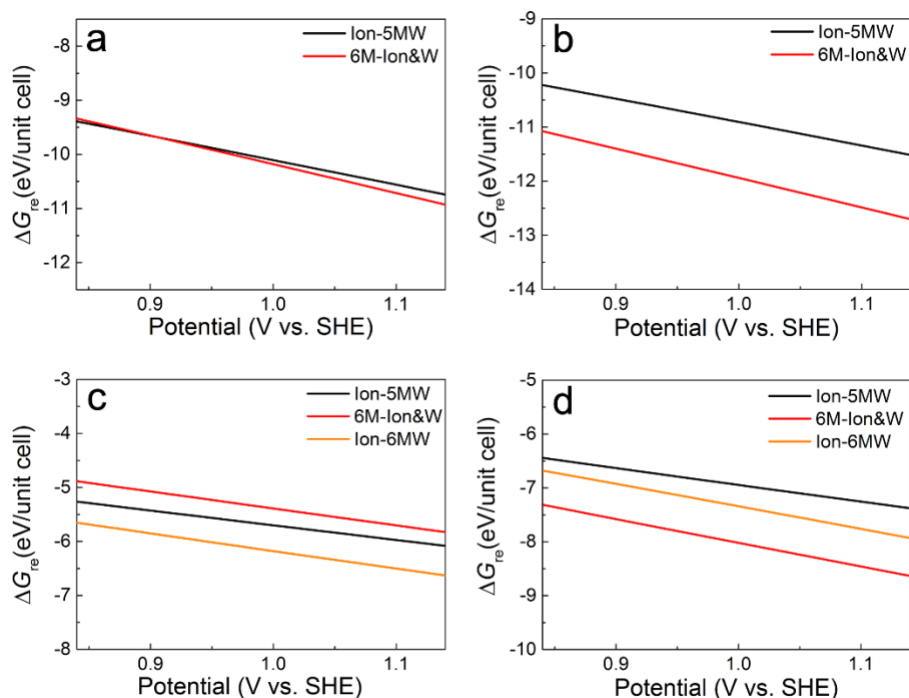
Fig. S13 Potential-dependent reaction free energies of different adsorbates combined with the 1st WL on Au(111)(3×5): (a) 2Py, (b) 2BS⁻, (c) PNBA⁻, and (d) BS⁻ from 0.84 to 1.14 V *vs*. SHE.

Table S1. STSs ($cm^{-1} V^{-1}$) of the EC-IR bands related to the adsorbed PNBA^{-a} from 0.84 to 1.14 V *vs*. SHE.

Modes	$\nu^{PNBA^-}_{anti-sym}(CO_2)$	$\nu^{PNBA^-}_{sym}(CO_2)$	$\nu^{PNBA^-}_{sym}(NO_2)$	$\nu^{PNBA^-}(CN)$
Expt.	12.72	12.98	12.68	-12.86
Ion-5MW	11.10	10.98	10.99	-11.01
6M-Ion&W	10.46	11.70	10.46	-10.35
Mol-5MW	-24.41	13.21	35.70	-10.71
Ion W/O W	–	–	6.22	-9.12

^{a}Detailed vibrational modes of $\nu^{PNBA^-}_{anti-sym}(CO_2)$, $\nu^{PNBA^-}_{sym}(CO_2)$, $\nu^{PNBA^-}_{sym}(NO_2)$, and $\nu^{PNBA^-}(CN)$ were listed in Fig. S6.

References

1 G. Kresse and J. Furthmuller, *Phys. Rev. B*, 1996, **54**, 11169-11186.

2 B. Hammer, L. B. Hansen and J. K. Nørskov, *Phys. Rev. B*, 1999, **59**, 7413-7421.

3 J. P. Perdew, K. Burke and Y. Wang, *Phys. Rev. B*, 1996, **54**, 16533-16539.

4 S. Grimme, S. Ehrlich and L. Goerigk, *J. Comput. Chem.*, 2011, **32**, 1456-1465.

5 G. Kresse and D. Joubert, *Phys. Rev. B*, 1999, **59**, 1758-1775.

6 J. Tersoff and D. R. Hamann, *Phys. Rev. B*, 1985, **31**, 805-813.

7 K. Mathew, R. Sundararaman, K. Letchworth-Weaver, T. Arias and R. G. Hennig, *J. Chem. Phys.*, 2014, **140**, 084106.

8 K. Mathew, V. S. C. Kolluru, S. Mula, S. N. Steinmann and R. G. Hennig, *J. Chem. Phys.*, 2019, **151**, 234101-234108.

9 R. Jinnouchi, T. Hatanaka, Y. Morimoto and M. Osawa, *Phys. Chem. Chem. Phys.*, 2012, **14**,

3208-3218.

10 Y. Fang, S. Y. Ding, M. Zhang, S. N. Steinmann, R. Hu, B. W. Mao, J. M. Feliu and Z. Q. Tian, *J. Am. Chem. Soc.*, 2020, **142**, 9439-9446.

11 H. Miyake, S. Ye and M. Osawa, *Electrochem. Commun.*, 2002, **4**, 973-977.

12 S.-G. Sun, W.-B. Cai, L.-J. Wan and M. Osawa, *J. Phys. Chem. B*, 1999, **103**, 2460-2466.

13 P. Lange, V. Glaw, H. Neff, E. Piltz and J. K. Sass, *Vacuum*, 1983, **33**, 763-766.